Strojniški vestnik - Journal of Mechanical Engineering vol(yyyy)no, p-p
DOI code
Original / Review / Short Scientific Paper
Received for review: yyyy-mm-dd
Received revised form: yyyy-mm-dd
Accepted for publication: yyyy-mm-dd
© 2015 Journal of Mechanical Engineering. All rights reserved.

Study on the dynamic characteristics of bit anchor cable drilling in gravel sediments of a soft rock bottom hole

Kuidong Gao[1,2], Jihai Liu[1,2*], Qingliang Zeng[3], Jingyi Cheng[4], Liqing Sun[1], Lisong Lin[1,2]
1. College of Mechanical and Electrical Engineering, Shandong University of Science and Technology, Qingdao 266590, China
2. Shandong Province Key Laboratory of Mine Mechanical Engineering, ShandongUniversity of Science and Technology, Qingdao 266590, China
3. School of Information Science and Engineering, Shandong Normal University, Jinan 250014, China
4. School of Mines, China University of Mining and Technology, Xuzhou 221116, China

During the pore-forming stage of floor heave treatment, the phenomenon of gravel sediment accumulation in the bottom hole often occurs, which causes great difficulties to the normal installation of the anchor cable. Based on this observation, a new anchor cable installation method was proposed, which involves installing a drill bit at the front end of the anchor cable to assist its drilling. With the help of the anchor cable drilling test bench, the influence of bit, motion parameters and hole environment on the performance of anchor cable drilling was studied. Through the co-simulation of discrete element method - multibody dynamics (DEM-MBD), the drilling process of the bit anchor cable was simulated, and the dynamic characteristics of the bit anchor cable drilling in the bottom hole gravel sediment were analyzed. The results show that installing a drill bit in front of the anchor cable can greatly reduce the drilling resistance and hinder torque during anchor cable drilling. When the rotational direction of the bit anchor cable is consistent with the spiral direction of the anchor cable, the bit anchor cable can exhibit better drilling performance. The drilling resistance and hindering torque of the bit anchor cable are the largest when drilling in soaked particles, followed by drilling in dry particles, and the smallest occurs when drilling in moist particles. The research results can provide reference for the parameter setting of anchor cable auxiliary installation equipment.

Keywords: Bit; Anchor cable; Gravel drilling; Dynamic characteristic

0 INTRODUCTION

Th stability control of soft rock roadways has always been a technical problem in coal mine production and construction, especially with floor heave in nonlinear large deformation control of soft rock roadways [1-3]. Floor heave will reduce the section size, hinder normal transportation, impede ventilation, and easily cause safety accidents in the roadway. Floor heave seriously restricts the safety and efficiency of coal mining [4-6].

As shown in Fig. 1, the main method used to solve the problem of roadway floor heave involves using the anchor cable to directly control the floor to maximize the radial stress of the floor rock mass [7-9]. However, due to the complexity and uncertainty of the floor rock mass, the phenomenon of hole wall instability easily appears in the pore-forming stage, resulting in the accumulation of gravel sediments in the bottom hole. This sediment accumulation will greatly hinder the normal installation of anchor cables. At present, the main solution to this problem is the manual installation of anchor cables, which manually controls the installation path of the anchor cable so that it can be installed close to the bottom of the borehole. However, the front end of the anchor cable is blunt, giving it a large installation resistance and low installation efficiency. In order to improve the installation efficiency of the anchor cable in the hole, auxiliary installation equipment of anchor cable was designed as shown in Fig. 4, and proposed a new installation method of anchor cable in the hole by installing drill bit at the front end of anchor cable.

Through numerical calculation, Fang Lin et al. [10] comparatively analyzed the variation characteristics of anchor cable structure displacement under static. Jian Li et al. [11] proposed a new pressure-type anchor cable with a precast anchor head. Zhigang Tao et al. [12] established the nonlinear thermomechanical coupling analysis model of the finite element structure of constant resistance by using ANSYS software. Keyou Shi et al. [13] and [14] predicted the law and degree of the anchoring force loss

*Corr. Author's Address: Name of institution, Address, City, Country, xxx.yyy@xxxxxx.yyy

through the established coupling calculation model. Zhongping Yang et al. [15] studied the variation of anchor cable tension by monitoring the tensile behavior of the selected anchor cable. Wang et al. [16] studied the mechanical properties of the anchor cable under the tension-torsion coupling effect by using the established three-dimensional computational model. Through the established seabed model, Hongbo Sun et al. [17] explored the relationship between the normal seabed friction coefficient and the anchor cable tension. At present, most of the research performed on anchor cables focuses on their properties and applications. There are relatively few studies on the installation of anchor cables in gravel sediments in bottom holes.

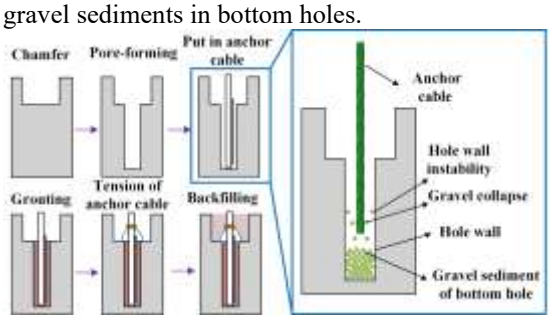

Fig. 1 *Background*

In 1971, Cundall P. A. first proposed an analysis method for discrete particles based on molecular dynamics theory [18-20], and then the method gradually developed into the discrete element method (DEM) [21-23]. The DEM method can construct the particle environment of a discrete material and can analyze the motion law of the particle under an external force [24-26]. However, the existing DEM software is weak in the mechanical analysis of the geometry in particles. This problem can be solved by discrete element method and multi-body dynamic method (DEM-MBD) cosimulation. Nowadays, The DEM-MBD co-simulation has been widely used in particle dynamics analysis [27], particle breakage experiment [28] and mechanical property analysis [29].

To explore the dynamic characteristics of drilling an anchor cable in the gravel sediments of bottom holes, an anchor cable drilling experiment was carried out with and without a drill bit by using the designed anchor cable drilling test bed. The gravel drilling experiments were performed using different motion parameters, hole diameters, particle humidities and particle types to obtain the dynamic characteristics of bit anchor cable drilling under various conditions. Additionally, DEM-MBD cosimulation was used to simulate the drilling process of the bit anchor cable in the gravel sediments of a bottom hole, and the movement law of the gravel particles in the hole was obtained by drilling the bit anchor cable under different motion parameters.

The research solves the difficulty of anchor cable installation caused by the accumulation of gravel in the hole. The anchor cable auxiliary installation equipment can solve the problems of low efficiency and high cost of manual installation of anchor cable. The effect of bit anchor cable on the motion of discrete particles is revealed by DEM-MBD. It is proved that the drilling process of bit anchor cable is also a process in which the stable structure of gravels is constantly broken and rebuilt. The favorable factors of bit anchor cable installation in the environment of gravel accumulation in the hole are obtained: bit anchor cable clockwise rotation, low forward speed, high rotational speed, moist gravel particles, particle diameter 10-13 mm and regular particle shape.

1 SIMULATION MODELS AND TEST

1.1 Simulation Model

The Hertz–Mindlin (no-slip) contact model is the most commonly used model in discrete element simulation. The Hertz–Mindlin model has the benefits of high accuracy and high computational efficiency. DEM-MBD is a common method for simulating the motion of geometry in discrete particles [27,29]. The schematic diagram of DEM is shown in Fig. 2(a). The co-simulation diagram of DEM-MBD is shown in Fig. 2(b). The contact forces between particles include the normal contact force, tangential contact force and friction force. The dynamic system of normal contact force and tangential contact force is a spring damping system. In DEM, it is assumed that the gravel has the same diameter and will not be damaged or deformed under the action of external forces. In MBD, it is assumed that the anchor cable is a rigid body. The anchor cable will not bend and change its motion state under the action of external forces.

When gravel sediments accumulate at the bottom of the hole, the most common solution is manual installation. The installation path of the

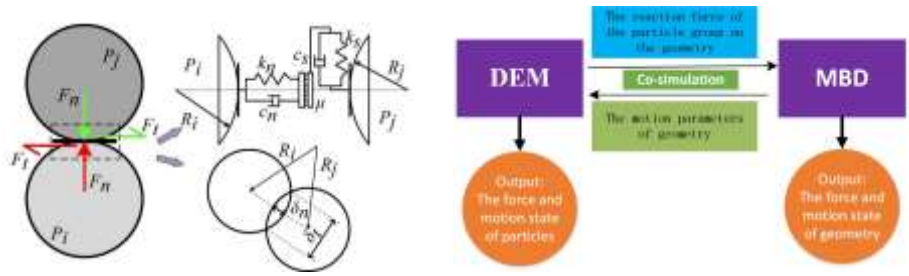

a) b)

Fig. 2 *Simulation Mode; a) IHertz–Mindlin (no-slip) contact model; b) DEM-MBD co-simulation model*

Where P_i is the discrete particle with radius R_i; P_j is the discrete particle with radius R_j; F_t is the tangential contact force, N; F_n is the normal contact force, N; K_s is the tangential elastic coefficient; K_n is the normal elastic coefficient; c_s is tangential damping coefficient; c_n is the normal damping coefficient; μ is the friction coefficient; δ_n is the overlap width of the particles, m; δ_t is the overlap length of the particles, m.

Table 1. *The parameters of DEM* [27].

	P (kg/m^3)	σ	G (GPa)		η	μ_S	μ_R
Gravel	2700	0.29	11	Gravel – Gravel	0.62	0.74	0.2
Anchor cable	7801	0.29	8.02	Gravel – Anchor cable	0.42	0.49	0.25

where ρ is the density, σ is Poisson's ratio, G is the shear modulus, η is the coefficient of restitution, μ_S is the coefficient of static friction, and μ_R is the coefficient of rolling friction.

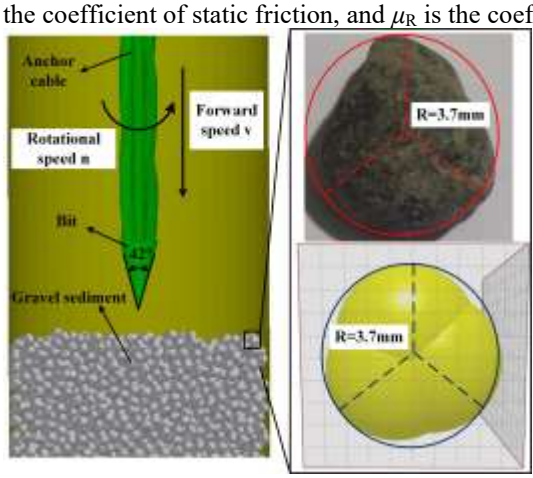

Fig. 3 *Simulation model of drilling bottom hole gravel with a bit anchor cable*

anchor cable is manually controlled so that the anchor cable can be installed near the bottom of the borehole. However, manual installation has its shortcomings because the front end of the anchor cable is blunt, the installation resistance of the anchor cable is large, the installation efficiency is low, and the technique is labor-intensive. Based on these disadvantages, a new anchor cable installation method was proposed, in which a drill bit was installed at the front end of the anchor cable so that the bit could assist the anchor cable drilling. The constructed simulation model of the bit anchor cable drilling into the bottom hole gravels is shown in Fig. 3.

1.2 Test Bed

In order to improve the installation efficiency of the anchor cable in the hole, auxiliary installation equipment of anchor cable was designed as shown in Fig. 4, and proposed a new installation method of anchor cable in the hole by installing drill bit at the front end of anchor cable. The core system of the auxiliary installation device is the clamping driveline and the rotary system. The clamping of anchor cable was realized by cylinder, and the rotary drilling of anchor cable was realized by two pneumatic motors.

According to the movement characteristics of the anchor cable when drilling in the gravel sediments of the bottom hole, the main structure of the anchor cable drilling test bed is shown in Fig. 5. The lead screw was driven by Motor 1 to rotate, thereby causing the vertical movement of Motor 2 and the anchor cable. The anchor cable clamp was driven by Motor 2 to rotate the anchor cable. Motor 1 and Motor 2 cooperated with each other so that the anchor cable could be drilled in the gravels in the bottom hole.

There were five kinds of gravel cylinders in total, and the diameters of the holes were 80, 120, 160, 200 and 240 mm. The sensor signals of the current transducer and pressure sensor were input into the DHDAS dynamic signal acquisition and

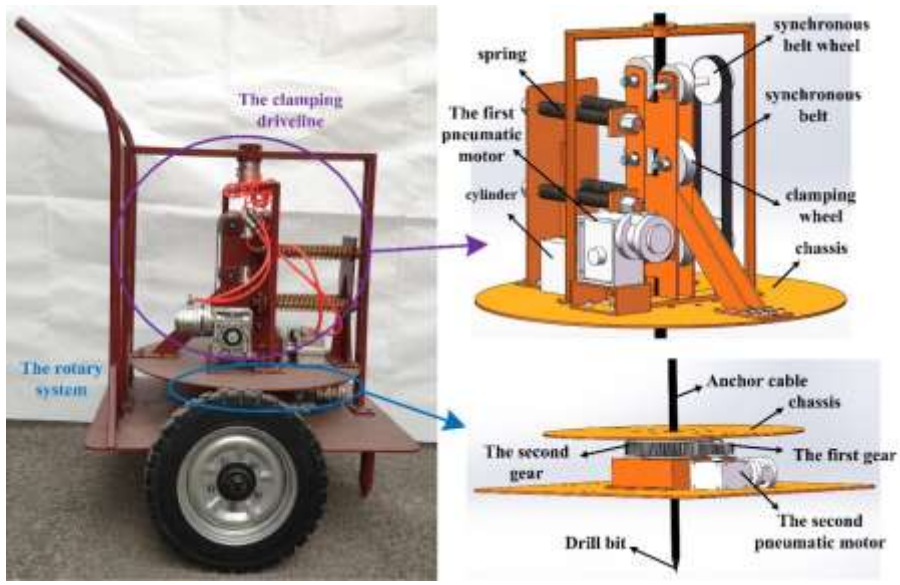

Fig.4 *Anchor cable auxiliary installation equipment*

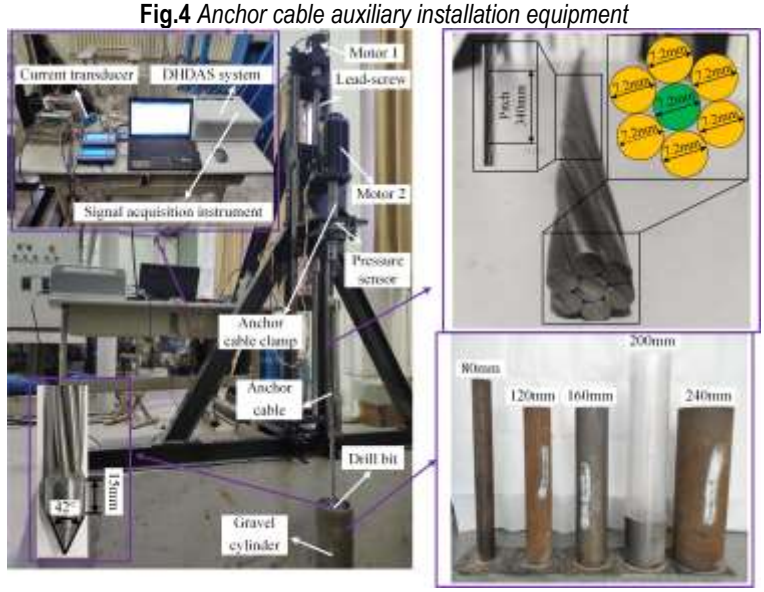

Fig. 5 *Anchor cable drilling test bed*

analysis system through a signal acquisition instrument. The sampling frequency of the system was 1000 Hz.

2 EXPERIMENT AND SIMULATION

Because the drilling depth and hindering torque of the anchor cable could not be measured directly through the experiment, the original data collected needed to be processed again. The current of Motor 2 could be collected through the current transducer, and the torque of Motor 2 could be obtained through Eq. (1). The torque of Motor 2 was also the total torque of the anchor cable. The drilling depth of the anchor cable could be obtained from Eq. (2), and the obstruction effect of gravel particles on the anchor cable could be obtained from Eq. (3).

$$T_1 = \frac{9550P_1}{n} = \frac{9.55\sqrt{3}UI}{n}\cos\varphi \quad (1)$$

where T_1 is the motor torque, N·m; P_1 is the power, W; n is the rotational speed of Motor 2, rpm; U is the voltage, V; I is the current, A; cosφ is the power factor.

$$h = P_2 t_1 \frac{n}{60} \tag{2}$$

where h is the drilling depth of the anchor cable, m; P_2 is the screw pitch of the lead screw, m. t_1 is the running time of motor 1, s.

$$T = T_1 - T_0 \tag{3}$$

where T_0 is the motor 2 torque when the drill bit just touches the particle, N·m.

2.1 Feasibility Study on Gravel Sediments Drilling with Bit Anchor Cable

To explore the influence of a drill bit installed on the front end of an anchor cable on drilling the gravel sediment in a bottom hole, gravel drilling experiments of an anchor cable with and without a drill bit were performed. The forward speed of the anchor cable was 0.01 m/s and the rotational speed was 60 rpm. The hole diameter of the gravel cylinder was 160 mm and the diameters of the gravel sediments were 3–6 mm. The experimental results are shown in Fig. 6.

Fig. 6 shows that installing a drill bit at the front end of the anchor cable can greatly reduce the braking effect of gravel particles on anchor cable drilling. Fig. 6(a) shows that at the same drilling depth, the drilling resistance of the anchor cable without a drill bit is the largest when it rotates counterclockwise, and the drilling resistance of the anchor cable with a drill bit is the smallest when it rotates clockwise.

Fig. 6(b) shows that when the drilling depth is less than 0.2 m, the hindering torque by counterclockwise rotation of the anchor cable without a bit is the largest, the clockwise rotation of the anchor cable without a bit is the second largest, and the clockwise rotation of the anchor cable with a bit is the smallest. However, when the drilling depth was greater than 0.2 m, the hindering torque by the clockwise rotation of the anchor cable without a bit increased rapidly. When the drilling depth was 0.21 m, the hindering torque reached 24 N·m. When the drilling depth was 0.25 m, the hindering torque reached the maximum value of 46 N·m, and Motor 2 stopped rotating directly under this torque.

The drilling process of clockwise rotation of the anchor cable without a bit is shown in Fig. 7. Because the anchor cable has a certain spiral

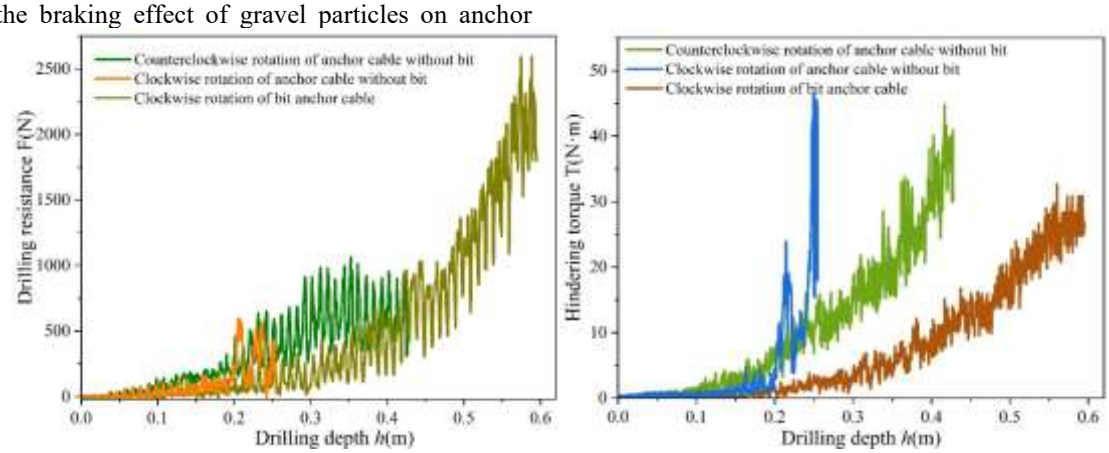

a) b)

Fig. 6 *Comparison diagram of anchor cable drilling; a) drilling resistance; b) hindering torque*

structure, when the rotational direction of the anchor cable was consistent with the spiral structure direction of the anchor cable, the spiral structure of the anchor cable would be untied under the action of an external force, which would cause a rapid increase in the hindering torque.

According to the results, when the anchor cable without a bit rotated clockwise to drill the gravel sediments in the bottom hole, the spiral structure of the anchor cable was damaged, which led to a rapid increase in the hindering torque. Although the anchor cable without a bit could complete the gravel drilling in the bottom hole by rotating counterclockwise, the resistance of the anchor cable drilling was large in the process. After the bit was installed at the front end of the anchor cable, the drilling resistance and hindering torque could be greatly reduced. Therefore, the

follow-up study focused on the dynamic characteristics of bit anchor cable gravel drilling.

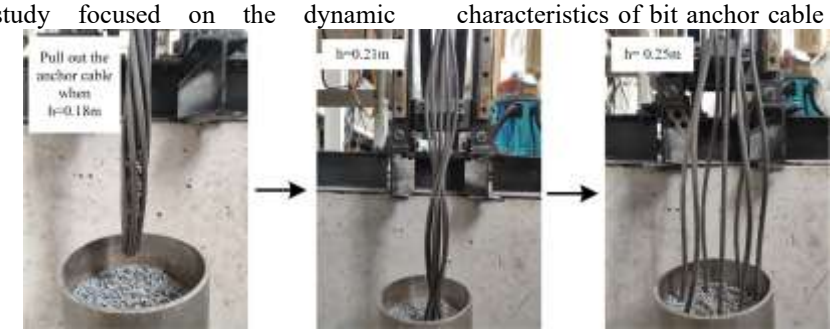

Fig. 7 *Drilling process during clockwise rotation of anchor cable without bit*

2.2 Influence of The Motion Parameters on The Dynamic Characteristics of Bit Anchor Cable Drilling

The process of drilling the gravel sediment in the bottom hole with the bit anchor cable primarily used two movements: the forward movement in the vertical direction and the rotary movement around the anchor cable. Because the anchor cable has a certain spiral structure, exploring the influence of the rotational direction and rotational speed on its drilling dynamic characteristics is of great importance.

2.2.1 Rotational Direction

To explore the influence of the rotational direction on the drilling dynamic characteristics of the bit anchor cable, drilling experiments were carried out under different rotational directions. The inner diameter of the gravel cylinder used in the experiment was 160 mm, the diameters of the gravel sediments were 3–6 mm, and the forward speed of the bit anchor cable was 0.02 m/s.

Because gravel particles have a certain fluidity, the drilling resistance and hindering torque during bit anchor cable drilling have a certain fluctuation. To facilitate a comparative analysis of the drilling resistance and hindering torque in different rotational directions, Savitzky–Golay smoothing was performed on the curves. Experimental curves after processing are shown in Fig. 8. Fig. 9 shows the average values of the drilling resistance and hindering torque in different rotation directions at drilling depths of 0.5-0.55 m.

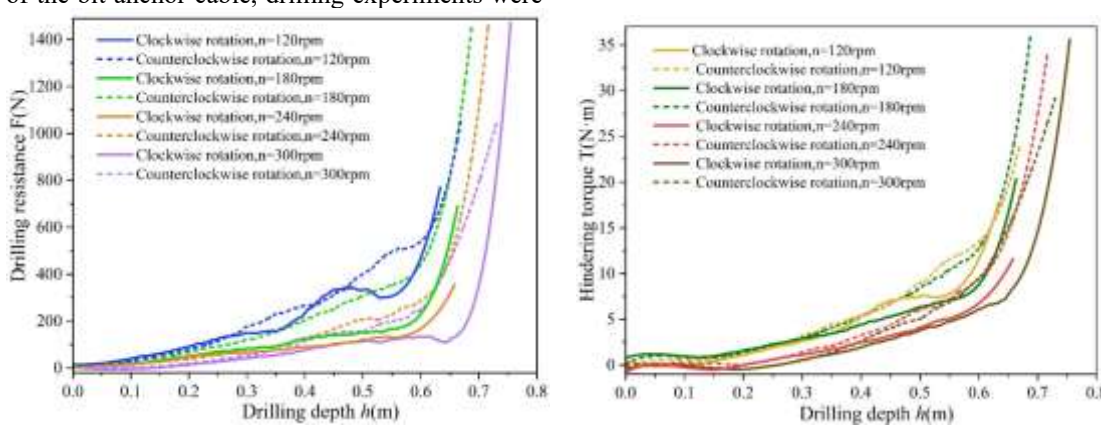

a) b)

Fig. 8 *The drilling curve of bit anchor cable; a) drilling resistance diagram; b) hindering torque diagram*

Fig. 8 and Fig. 9 show that with increasing drilling depth, the drilling resistance and hindering torque of the bit anchor cable during clockwise and counterclockwise rotation increased gradually. At the same rotational speed, clockwise rotation was less hindered by particles. The drilling resistance during clockwise rotation of the bit anchor cable was much less than that of counterclockwise rotation. When the drilling depth was 0.5-0.55 m, the drilling resistance under clockwise rotational speeds of 120, 180, 240 and 300 rpm was 36.5%, 52%, 43.6% and 34.9% lower than that of counterclockwise

rotation, respectively. This phenomenon was caused by the spiral structure of the anchor cable.

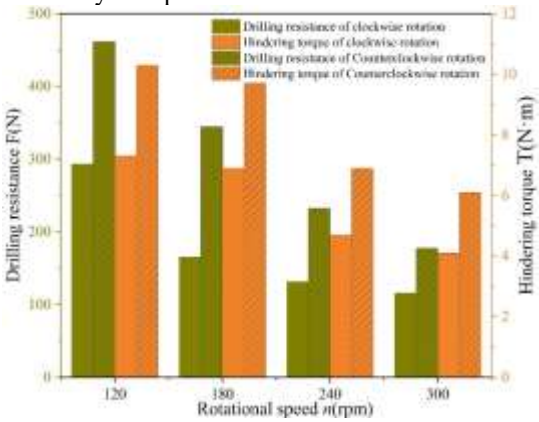

Fig. 9 *Average value of drilling resistance and hindering torque at 0.5-0.55 m*

To explore the influence of the anchor cable spiral structure on gravel particle movement during bit anchor cable drilling, the simulation model in Fig. 3 was numerically simulated by using DEM-MBD cosimulation. When the forward speed was 0.02 m/s, the bit anchor cable rotated clockwise at 120, 240 and 360 rpm and counterclockwise at 120, 240 and 360 rpm to simulate the drilling of gravel sediments in a bottom hole. The drilling resistance curves after Savitzky–Golay smoothing are shown in Fig. 10 a). When the bit anchor cable was drilled at a forward speed of 0.02 m/s and a rotational speed of 240 rpm, the comparison of drilling resistance between simulation and experiment is shown in Fig. 10 b), and the comparison of fitting slope is shown in Table 2.

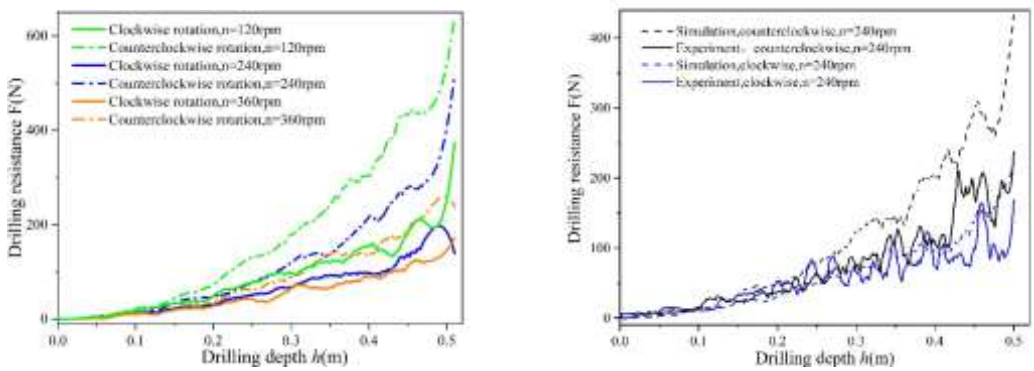

a) b)

Fig. 10 *Drilling resistance simulation curve*; a) *different rotational directions and rotational speeds; b) Comparison of simulation and experiment*

Table 2. *The fitted slope of drilling resistance.*

Condition	Rotational Direction	Slope	K_2/K_1
Experiment	Clockwise rotation	K_1=222.1	1.2
Simulation	Clockwise rotation	K_2=267.3	
Experiment	Counterclockwise rotation	K_1=310.1	1.6
Simulation	Counterclockwise rotation	K_2=491.3	

It can be seen that although the simulation drilling resistance was generally larger than the experimental drilling resistance, the change trend of drilling resistance was the same under different drilling depths, different rotational directions and different rotational speeds. Therefore, it was convincing to explain the variation rule of drilling resistance in the process of bit anchor cable drilling through DEM-MBD co-simulation.

Fig. 11 is the motion vector diagram of gravel particles around the anchor cable under different rotational directions when the drilling depth reached 0.4 m. It can be clearly seen from the figure that when the rotational direction of the anchor cable was clockwise, the rotation of the anchor cable would give an oblique upward thrust to the surrounding particles. When the rotational direction of the anchor cable was counterclockwise, the rotation of the anchor cable would give an oblique downward thrust to the surrounding particles.

When the anchor cable gave the gravel particles an oblique upward thrust, the anchor cable was subjected to the oblique downward reaction force of the gravel particles, so the drilling resistance of the bit anchor cable was

reduced. When the anchor cable gave the gravel particles an oblique downward thrust, the anchor cable was subjected to the oblique upward reaction force of the gravel particles, so the drilling resistance of the bit anchor cable was increased.

From the above results, it can be seen that clockwise rotation of the bit anchor cable could greatly reduce the drilling resistance and hindering torque during drilling compared to counterclockwise rotation of the bit anchor cable. Therefore, in the following experiments, the rotational direction of the bit anchor cable was clockwise.

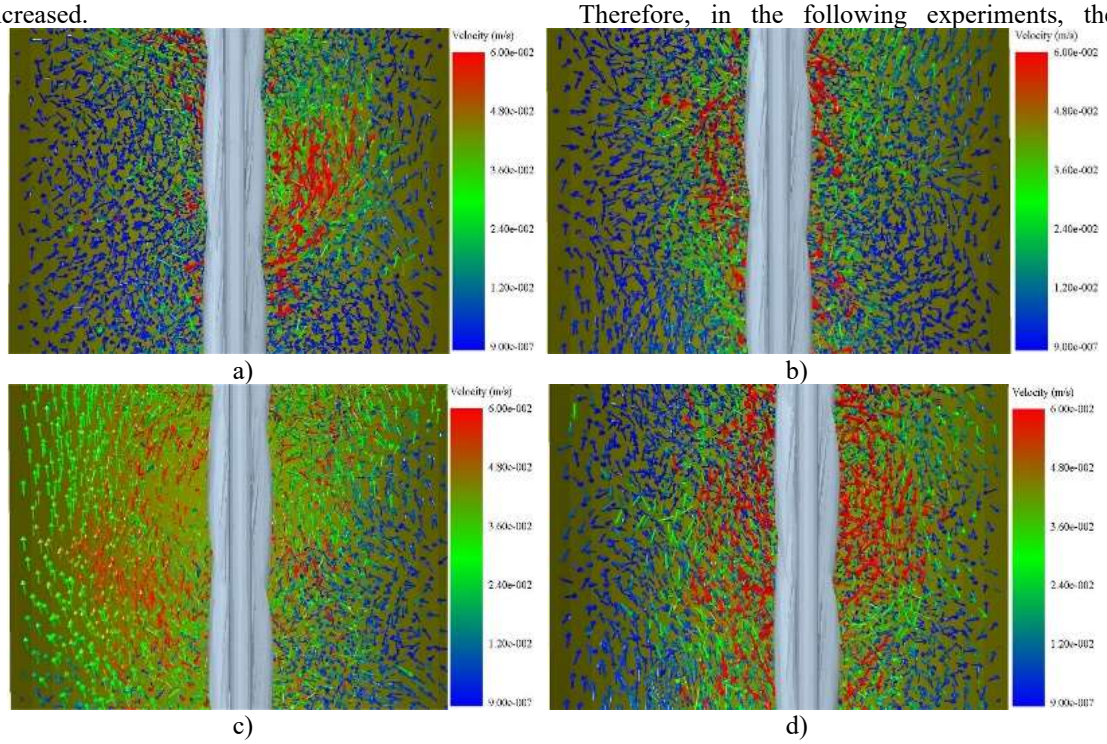

Fig. 11 *Motion state vector diagram of gravel particles under different rotational directions; a) clockwise 240 rpm; b) counterclockwise 240 rpm; c) clockwise 360 rpm; d) counterclockwise 360 rpm*

2.2.2 Rotational Speed

Fig. 8 shows that with increasing drilling depth, the drilling resistance and hindering torque of the bit anchor cable increased slowly at first and then rapidly. The drilling resistance and hindering torque of the bit anchor cable was inversely proportional to the rotational speed. It can be seen from Fig. 9 that the average drilling resistance and the average hindering torque of the bit anchor cable at the clockwise rotational speed of 300 rpm were 62.7% and 43.1% lower than those at the clockwise rotational speed of 120 rpm.

Fig. 11(a) and (c) shows that with increasing rotational speed, the number and velocity of particles moving upward gradually increased so that the downward thrust of particles to the anchor cable spiral structure gradually increased. Therefore, the drilling resistance of the bit anchor cable in Fig. 8(a) gradually decreased with increasing rotational speed.

When the bit anchor cable was drilled to the bottom hole at a forward speed of 0.02 m/s, the velocity vector of gravel sediment was shown in Fig. 12. With the increase in the rotational speed of the bit anchor cable, the particle movement of the gravel in the bottom hole became increasingly intense. When the rotational speed reached 240 rpm and 360 rpm, the particles with velocities greater than 0.024 m/s presented an obvious spiral distribution, and their rotational direction was consistent with the rotational direction of the bit anchor cable.

Therefore, when the bit anchor cable rotated in the gravel sediments of the bottom hole, the bit anchor cable could stir the gravels, and the faster the rotational speed was, the more obvious the stirring effect. The stirring effect of the bit anchor cable on gravel particles can reduce the drilling

resistance in the process of bit anchor cable drilling and allow for uniform mixing of the anchoring agent in the gravel sediments of the bottom hole in the later stage.

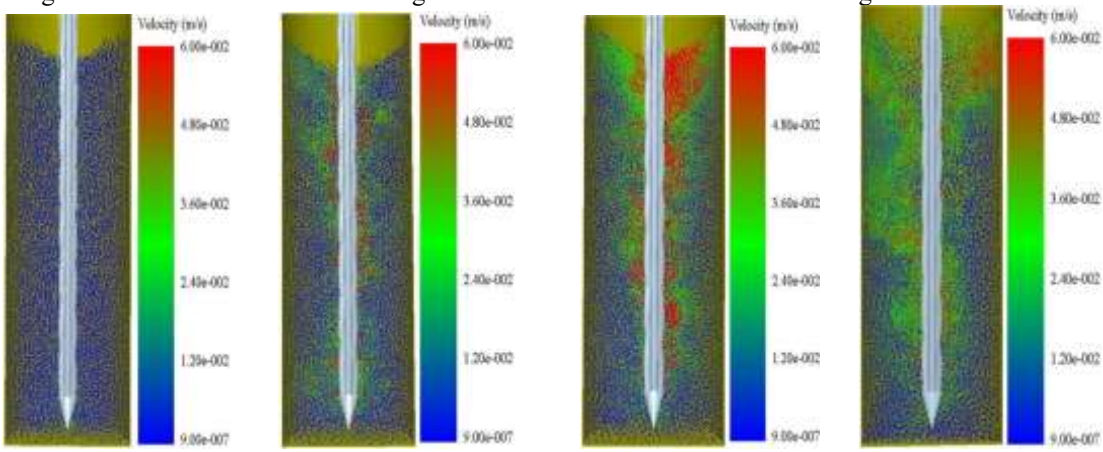

a) b) c) d)

Fig. 12 *Velocity vector diagram of gravel in the bottom hole at different rotational speeds; a) n=0 rpm; b) n=120 rpm; c) n=240 rpm; d) n=360 rpm*

2.3 Influence of particle moisture on the dynamic characteristics of bit anchor cable drilling

2.3.1 Moist Particle

In the actual installation process of the anchor cable, the gravel in the hole was not completely dry, so to make the experimental environment closer to the real working conditions, drilling experiments were carried out on gravel particles with different moisture contents. The forward speed of the bit anchor cable was 0.025 m/s, and the gravel state was 3-6 mm particle after 12 h immersion. After Savitzky–Golay smoothing, the drilling resistance and hindering torque of the bit anchor cable when drilling in moist gravel particles were found, and the values are shown in Fig. 13.

Fig. 13 shows that, at the same rotational speed, the drilling resistance and hindering torque of the bit anchor cable when drilling in moist gravel particles were smaller than the values obtained when drilling in dry gravel particles. The reason for this phenomenon was related to the water molecules on the surface of the gravel particles. When the gravel particles were moist, a large number of water molecules were attached to the surface of the gravel particles, and then water film formed on the surface of the gravel particles, which reduced their surface friction coefficient. Thus, the drilling resistance and hindering torque of the bit anchor cable were reduced.

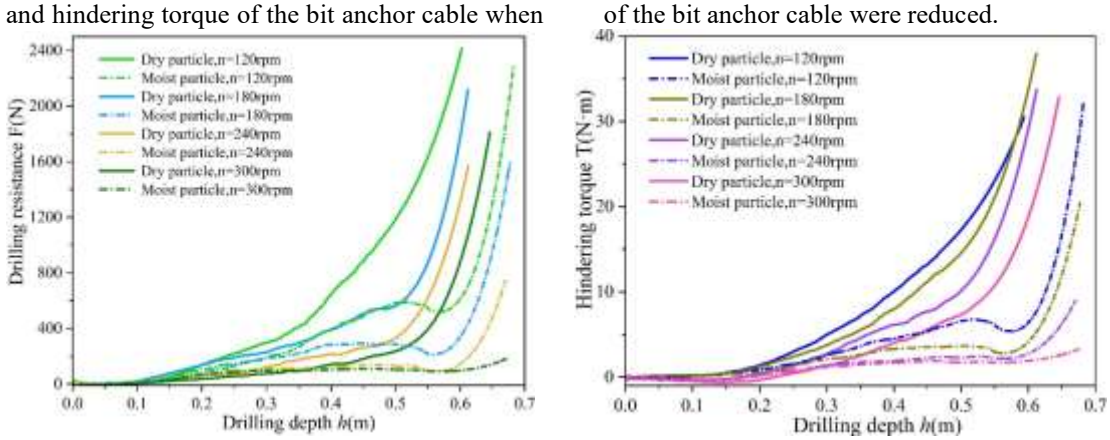

a) b)

Fig. 13 *Dynamic characteristic curve of moist gravel drilling; a) drilling resistance; b) hindering torque*

Fig. 13(b) shows that the hindering torque of the bit anchor cable drilling at 120 rpm in moist gravel particles was lower than that drilling at 300 rpm in dry gravel particles. Therefore, in practical

work, we can reduce the difficulty of bit anchor cable installation by improving the humidity of the gravel sediment, and the effect is more obvious than increasing the rotational speed of the bit anchor cable.

2.3.2 Soaked Particle

To further explore the influence of particle humidity on the dynamic characteristics of bit anchor cable drilling, gravel drilling was carried out on gravel particles completely soaked in water. Fig. 14 shows the drilling experiment diagram of soaked particles. The diameters of gravel were between 6-9 mm, and the forward speed of the bit anchor cable was 0.025 m/s. The drilling resistance and hindering torque of the bit anchor cable are shown in Fig. 15.

Fig. 15 shows that when the rotational speed was the same, the drilling resistance and hindering torque of the bit anchor cable when drilling in soaked particles were greater than those values found when drilling in dry gravel particles. When the particle diameters were 6-9 mm, the drilling resistance of the bit anchor cable when drilling in soaked particles at 300 rpm was higher than the drilling resistance obtained when drilling in dry particles at 120 rpm, which is substantially different from the trend found when drilling in moist gravel particles.

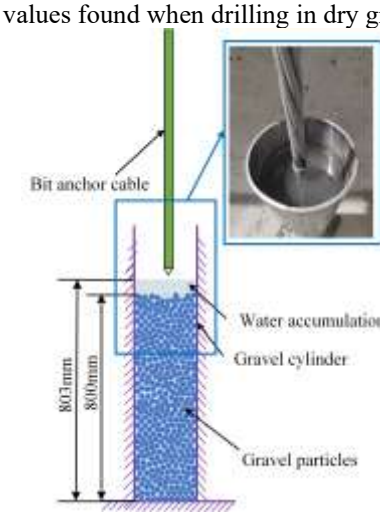

Fig. 14 *Drilling in soaked particles*

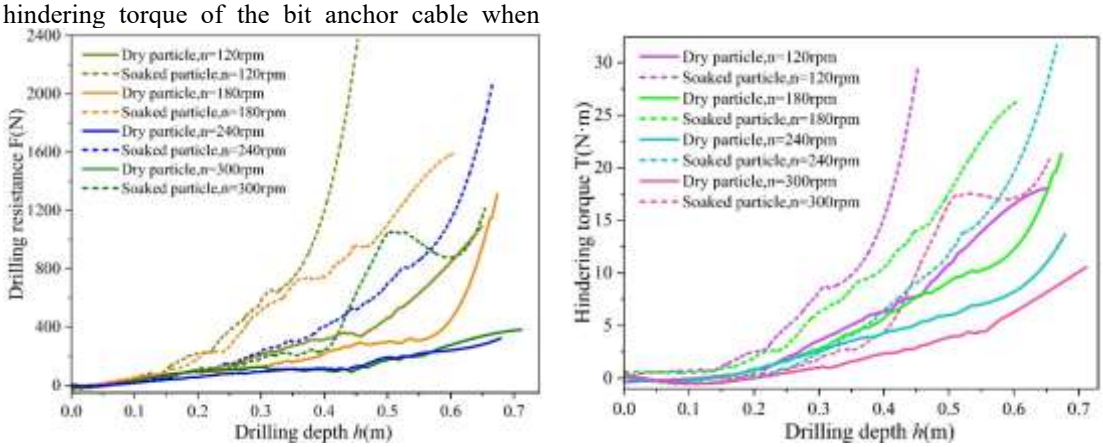

a) b)

Fig. 15 *Dynamic characteristic curve of soaked particle drilling; a) drilling resistance; b) hindering torque*

The reason for the above phenomenon relates to the amount of water in the hole. When there was less water in the hole, the friction coefficient between gravel particles could be reduced by water attaching to the surface of gravel particles, and then the drilling resistance and hindering torque of the bit anchor cable could be reduced. However, when there was too much water in the hole, the excessive water hindered the movement of gravel particles and increased the drilling resistance and hindering torque of the bit anchor cable. Therefore, excessive water in the hole should be avoided during bit anchor cable drilling; otherwise, the drilling resistance and hindering torque of the bit anchor cable will be significantly increased.

Meanwhile, Fig. 15 shows that when the bit anchor cable was drilled in the soaked particles at a rotational speed of 300 rpm and the drilling depth reached 0.5 m, the drilling resistance and hindering torque of the bit anchor cable increased significantly. The drilling resistance was 446% and the hindering torque was 400% of 0.4 m. When the bit anchor cable was drilled, the stable structure of the gravel particles was constantly rebuilt and broken. Drilling depths of 0.4-0.6 m fully reflected the process. When the drilling

depth was 0.4-0.5 m, the stability of the whole particle begins to reorganize, and when the drilling depth reached 0.5 m, the whole particle reached a stable state. 0.5-0.6 m was a process in which the stable state of particles was gradually broken. In this process, the sound of friction between bit anchor cable and gravel was very obvious.

2.4 Influence of particle type on the dynamic characteristics of bit anchor cable drilling

2.4.1 Particle Diameter

Due to the different rock strata, the types of gravel sediment in different areas are also quite different. As shown in Fig. 16, different types of gravel particles in different areas were collected, with gravel diameters of 3–6, 6–9 and 10–13 mm. Then, the bit anchor cable was used to drill different types of gravel particles at a forward speed of 0.025 m/s. The influence of the particle diameter on the drilling resistance and hindering torque of the bit anchor cable is shown in Fig. 17. The diameter of the gravel cylinder was 160 mm.

Fig. 16 Gravel particles of different diameters

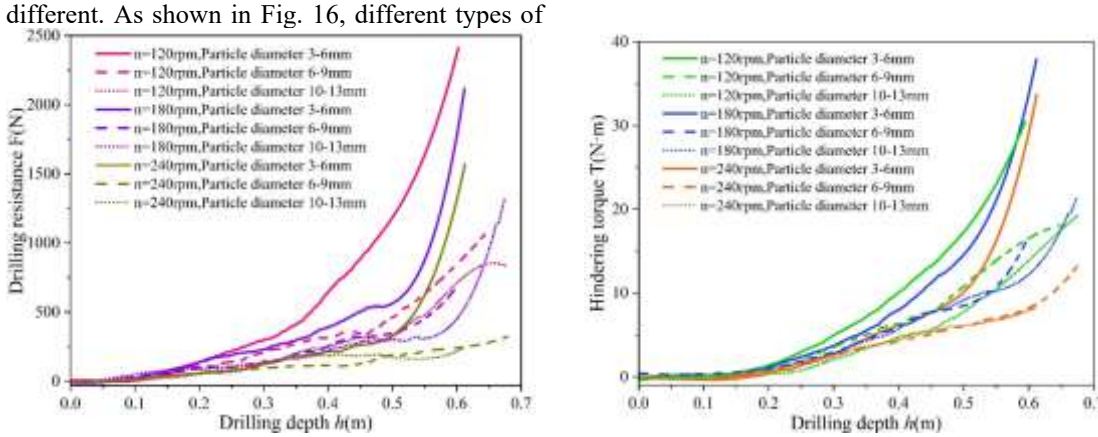

a) b)

Fig. 17 *Dynamic characteristic curve of the bit anchor cable drilling under different particle diameters; a) drilling resistance; b) hindering torque*

Fig. 17 shows that at the same rotational speed, with increasing gravel diameter, the drilling resistance and hindering torque of the bit anchor cable gradually decreased, and when the gravel diameter changed from 3–6 mm to 6–9 mm, the reduction in the drilling resistance and hindering torque of the bit anchor cable was much higher than that when the gravel diameter changed from 6–9 mm to 10–13 mm. The relationship between the diameter of gravel particles and the drilling resistance and hindering torque of the bit anchor cable was not a simple linear inverse ratio. Therefore, in real-world scenarios, when the diameter of the gravel in the hole is small, it is necessary to further improve the rotational speed of the bit anchor cable to ensure the same drilling efficiency.

2.4.2 Particle shape

The gravel sediment in the bottom hole is not only different in diameter but also in shape. To explore the influence of particle shape on the dynamic characteristics of bit anchor cable drilling, drilling experiments were carried out on the particles in Fig. 18 at a forward speed of 0.025 m/s. The experimental results following Savitzky–Golay smoothing are shown in Fig. 19.

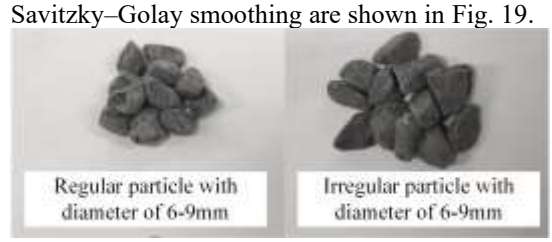

Fig. 18 *Gravel particles of different shapes*

Fig. 19 shows that under the same rotational speed, the drilling resistance and hindering torque of the bit anchor cable when drilling in regular gravels were less than those when drilling in irregular gravels. When the shape of the particle

was more regular, the rolling friction coefficient of the particle was smaller. In the same external environment, its motion state was easier to change, and it was easier to roll. Therefore, when the bit anchor cable was drilling in regular particles, the number of particles with rolling friction between the particles and the bit anchor cable was greater, and the number of particles with sliding friction was lower. As a result, drilling in regular particles was less difficult than drilling in irregular particles.

At the same time, the influence of the particle shape on the drilling resistance and hindering torque of the bit anchor cable decreased gradually with increasing rotational speed. Therefore, when the particle shape in the hole is irregular, the influence of particle shape on bit anchor cable drilling can be reduced by increasing the rotational speed of the bit anchor cable.

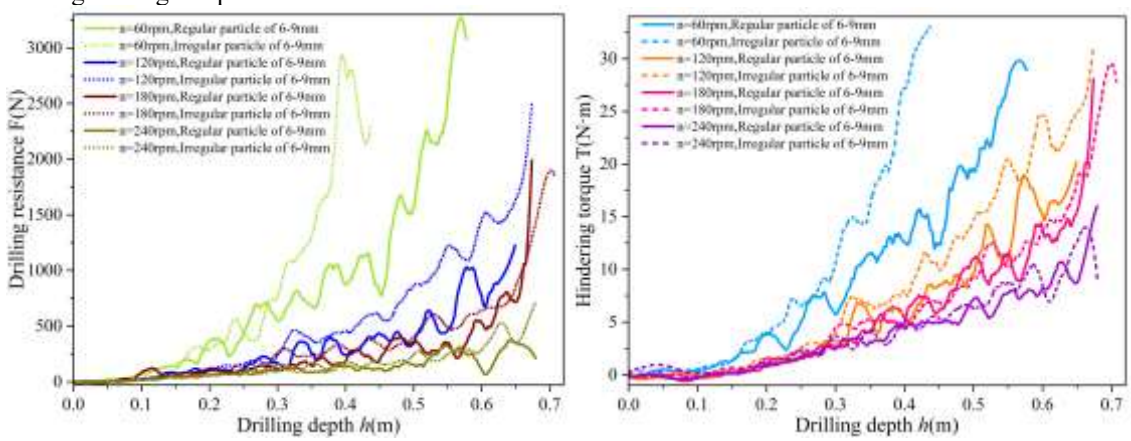

a) b)

Fig. 19 *Dynamic characteristic curve of bit anchor cable drilling under different particle shapes; a) drilling resistance; b) hindering torque*

3 CONCLUSIONS

In view of the difficulty of anchor cable installation caused by the accumulation of gravel sediment in the bottom hole, the auxiliary installation equipment of anchor cable was designed. And a new anchor cable installation method was proposed, which works by installing a drill bit in front of the anchor cable so that the drill bit could assist anchor cable drilling. The feasibility of this method was explored with an anchor cable drilling test bed. At the same time, the drilling process of the bit anchor cable in the gravel sediments in a bottom hole was simulated by DEM-MBD cosimulation. The main conclusions were as follows:

(1) When the anchor cable was drilled clockwise without the bit, the drilling depth was only 0.25 m. When the bit was installed in front of the anchor cable, the drilling depth was 0.6 m. Installing a bit in front of the anchor cable could significantly reduce the drilling resistance and hindering torque during anchor cable drilling. Clockwise drilling of the bit anchor cable was more beneficial to anchor cable installation than counterclockwise drilling. The drilling resistance and hindering torque of the bit anchor cable were inversely proportional to its rotational speed. The stirring effect of bit anchor cable drilling on gravel particles provides the possibility of uniform mixing of the anchor agent in the gravel sediments in a bottom hole.

(2) The drilling resistance and hindering torque of the bit anchor cable were the largest when drilling in soaked particles, followed by drilling in dry particles, and the smallest when drilling in moist particles. Therefore, during the installation of the bit anchor cable, the gravel should be kept moist as much as possible, but excessive water in the hole should be avoided. When the stable structure of gravel particles was broken or rebuilt, the drilling resistance and hindering torque of bit anchor cable could change greatly. When the bit anchor cable was drilled at 300 rpm in the soaked particles, the drilling resistance and hindering torque at 0.5 m were 446% and 400% of those at 0.4 m, respectively.

(3) The drilling resistance and hindering torque of the bit anchor cable were inversely proportional to the diameter of the gravel particles. In the experiment, the best drilling effect was achieved when the diameter of gravel particle was 10-13 mm. Compared with drilling in irregular gravels, drilling in regular gravels could make the bit anchor cable have less drilling resistance and hindering torque. The influence of particle shape on bit anchor cable drilling decreased with increasing rotational speed. Therefore, when the gravel diameter is small and the shape is irregular, it is necessary to further improve the rotational speed of the bit anchor cable to ensure the same installation efficiency.

4 ACKNOWLEDGEMENTS

The project was supported by the National Natural Science Foundation of China (Grant No.52174146) and the Project of Shandong Province Higher Educational Young Innovative Talent Introduction and Cultivation Team (Performance enhancement of deep coal mining equipment).

5 REFERENCES

[1] Hao, W., Tao, D. (2019). Research on Deformation Control Technology of Broken Soft Rock Pre-mining Roadway. *IOP Conference Series: Earth and Environmental Science*, vol. 358, no. 4, DOI:10.1088/1755-1315/358/4/042047.

[2] Sun, Y., Li, G., Zhang, J., Xu, J. (2020). Failure mechanisms of rheological coal roadway. *Engineering Failure Analysis*, vol. 12, no. 7, DOI:10.3390/su12072885.

[3] Gao, Y., Wang, C., Liu, Y., Wang, Y., Han, L. (2021). Deformation Mechanism and Surrounding Rock Control in High-Stress Soft Rock Roadway: A Case Study. *Advances in Civil Engineering,* vol. 2021, DOI:10.1155/2021/9950391.

[4] Xu, Y., Pan, K., Zhang, H. (2019). Investigation of key techniques on floor roadway support under the impacts of superimposed mining: theoretical analysis and field study. *Environmental Earth Sciences*, vol. 78, no. 15, DOI:10.1007/s12665-019-8431-9.

[5] Du, M., Wang, X., Zhang, Y., Li, L., Zhang, P. (2020). In-situ monitoring and analysis of tunnel floor heave process. *Engineering Failure Analysis*, vol. 109, no. 9, p. 104323, DOI:10.1016/j.engfailanal.2019.104323.

[6] Lai, X., Xu, H., Shan, P., Wang, Y., Zeyand, Wu, X., (2020). Research on Mechanism and Control of Floor Heave. *Energies.* DOI:10.3390/en13020381.

[7] Wu, G., Yu, W., Zhang, J., Ning, Y. (2017). Control Mechanism and Support Technology of Soft Coal Roadway in the Fully Mechanized Mining Work Face. *Geo-Resources Environment and Engineering*, vol. 2, p. 211–217, DOI:10.15273/gree.2017.02.038.

[8] Zhao, C.X., Li, Y.M., Liu, G., Meng, X., (2017). Mechanism analysis and control technology of surrounding rock failure in deep soft rock roadway. *Engineering Failure Analysis*, vol. 115, p. 104611, DOI:10.1016/j.engfailanal.2020.104611.

[9] Shi, L., Zhang, H., Wang, P. (2020). Research on Key Technologies of Floor Heave Control in Soft Rock Roadway. *Advances in Civil Engineering*, vol. 2020, DOI:10.1155/2020/8857873.

[10] Lin, F., Mengjun, W., Guangdi, W., Peng, C. (2016). Comparative Analysis on Stress State of Submerged Floating Tunnels in Different Anchor Cable Arrangement Modes. *Procedia Engineering,* vol. 166, p. 279–287, DOI:10.1016/j.proeng.2016.11.550.

[11] Li, J., Li, L. (2016). Numerical analysis on a new pressure-type anchor cable with precast anchor head based on FLAC3d. *Icence*, p. 237–241, DOI:10.2991/icence-16.2016.51.

[12] Tao, Z. (2018). Static tension test and the finite element analysis of constant resistance and large deformation anchor cable. *Advances in Mechanical Engineering*, vol. 10, no. 12, p. 1–13, DOI:10.1177/1687814018810638.

[13] Shi, K., Wu, X., Liu, Z., Dai. S. (2019). Coupled calculation model for anchoring force loss in a slope reinforced by a frame beam and anchor cables. *Engineering Geology*, vol. 260, p. 105245, DOI:10.1016/j.enggeo.2019.105245.

[14] Shi, K., Wu, X., Tian, Y., Xie, X. (2021). Analysis of re-tensioning time of anchor cable based on new prestress loss model. *Mathematics*, vol. 9, no. 10, DOI:10.3390/math9101094.

[15] Yang, Z., Li, S., Yu, Y., Liu, X., Hu, Y. (2020). Study on the variation characteristics of the anchor cable prestress based on field monitoring in a foundation pit. *Arabian Journal of*

Geosciences, vol. 13, no. 23, DOI:10.1007/s12517-020-06264-z.

[16] Wang, S.R., Wang, Z.L., Chen, Y.B., Wang, Y.H., Huang, Q.X. (2020). Mechanical performances analysis of tension-torsion coupling anchor cable. *International Journal of Simulation Modelling*, vol. 19, no. 2, p. 231–242, DOI:10.2507/IJSIMM19-2-512.

[17] Sun, H.G., Chen, G. (2021). Dynamic model of cable tension and configuration for vessel at anchor. *Journal of Marine Science and Technology*, vol. 26, no. 4, p. 1144–1152, DOI:10.1007/s00773-021-00802-4.

[18] Kim. Y.M. (2008). A Granular motion simulation by discrete element method. *Journal of Mechanical Science and Technology*, vol. 22, no. 4, p. 812–818, DOI: 10.1007/s12206-008-0112-7.

[19] Siegmann, E., Jajcevic, D., Radeke, C., Strube, D., Friedrich, K., Khinast, J.G. (2017). Efficient Discrete Element Method Simulation Strategy for Analyzing Large-Scale Agitated Powder Mixers. *Chemie-Ingenieur-Technik*, vol. 89, no. 8, p. 995–1005, DOI:10.1002/cite.201700004.

[20] Mitsufuji, K., Nambu, M., Hirata, K., Miyasaka, F. (2018). Numerical method for the ferromagnetic granules utilizing discrete element method and method of moments. *IEEE Transactions on Magnetics*, vol. 54, no. 3, p. 3–6, DOI:10.1109/TMAG.2017.2758799.

[21] Lee, Y.S., Nandwana, P., Zhang, W. (2018). Dynamic simulation of powder packing structure for powder bed additive manufacturing. *International Journal of Advanced Manufacturing Technology*, vol. 96, no. 1–4, p. 1507–1520, DOI:10.1007/s00170-018-1697-3.

[22] Wang, X., Li, B., Yang, Z. (2018). Analysis of the Bulk Coal Transport State of a Scraper Conveyor Using the Discrete Element Method. *Strojniški vestnik-Journal of Mechanical Engineering*, Vol. 64, no. 1, p. 37-46, DOI:10.5545/sv-jme.2017.4790.

[23] Yan, H., Li, Y., Yuan, F., Peng, F. (2020). Analysis of the Screening Accuracy of a Linear Vibrating Screen with a Multi-layer Screen Mesh. *Strojniški vestnik-Journal of Mechanical Engineering*, Vol. 66, no. 5, p. 289-299. DOI:10554/sv-jme.2019.6523.

[24] Wang, Z., Li, B., Liang, C., (2021). Response Analysis of a Scraper Conveyor under Chain Faults Based on MBD-DEM-FEM. *Strojniški vestnik - Journal of Mechanical Engineering*, Vol. 67, no. 10, p. 501-515.DOI:10.5545/sv-jme.2021.7300.

[25] Z, Y., S, X.X., M, W.J. (2021). Research on the axial velocity of the raw coal particles in vertical screw conveyor by using the discrete element method. *Journal of Mechanical Science and Technology*, vol. 35, no. 6, p. 2551–2560, DOI:10.1007/s12206-021-0526-z.

[26] Liu, H., Zhang, S.H., Ding, Y.P., Shi, G.L., Geng, Z. (2021). A simplified formulation for predicting wrinkling of thin-wall elbow tube in granular media–based push-bending process. *International Journal of Advanced Manufacturing Technology*, vol. 115, no. 1–2, p. 541–549, DOI:10.1007/s00170-021-07168-2.

[27] Gao, K., Liu, J., Wu, T., Zeng, Q., Sun, L., Zhang, X. (2022). Drilling study of bit in gravel environment based on DEM–MBD. *Engineering Reports*, vol. 4, no. 4, p. 1–21, DOI:10.1002/eng2.12472.

[28] Shi, S., Gao, L., Xiao, H., Xu, Y., Yin, H. （2021）. Research on ballast breakage under tamping operation based on DEM–MBD coupling approach. *Construction and Building Materials*, vol. 272, p. 121810, DOI:10.1016/j.conbuildmat.2020.121810.

[29] Chen, Z., Xue, D., Wang, G., Cui, D., Fang, Y., Wang, S. (2021). Simulation and optimization of the tracked chassis performance of electric shovel based on DEM-MBD. *Powder Technology*, vol. 390, p. 428–441, DOI:10.1016/j.powtec.2021.05.085.